Spectral shift response of optical whispering-gallery modes due to water vapor adsorption and desorption

2010 Meas. Sci. Technol. 21 115206

(http://iopscience.iop.org/0957-0233/21/11/115206)

Meas. Sci. Technol. **21** (2010) 115206 (7pp) doi:10.1088/0957-0233/21/11/115206

Spectral shift response of optical whispering-gallery modes due to water vapor adsorption and desorption

Qiulin Ma, Lei Huang, Zhixiong Guo and Tobias Rossmann[1]

Department of Mechanical and Aerospace Engineering, Rutgers, The State University of New Jersey, Piscataway, NJ 08854, USA

E-mail: rossmann@jove.rutgers.edu

Received 3 May 2010, in final form 28 July 2010
Published 18 October 2010
Online at stacks.iop.org/MST/21/115206

Abstract
The spectral shift response of optical whispering-gallery modes due to the adsorption and desorption of water molecules into a SiO_2 nano-coating is investigated. This coating is applied to a silica microsphere and optical-shift measurements are made at a very low humidity level (<10%). The micro-optical coupling system is incorporated into a sealed vacuum chamber for controlled humidity testing. The experimental observation of the whispering-gallery-mode spectral shift with refractive index is consistent with a theoretical analysis using Mie theory. A significant hysteresis effect is observed in the spectral shift of individual whispering-gallery modes during variable humidity tests. To understand the hysteresis mechanism, tests with step changes in humidity are performed, which reveal complex and dynamic water molecule transport phenomena between the nano-coating and surrounding environment.

Keywords: whispering-gallery mode, humidity sensor, water vapor concentration, optical resonance shift, ultra-fine resolution

(Some figures in this article are in colour only in the electronic version)

1. Introduction

Optical whispering-gallery-mode (WGM) effects in dielectric micro-resonators such as microspheres [1–4], microdisks [5, 6] or microrings [7] have been intensively investigated for the development of new biological and/or chemical sensors. The WGMs correspond to the total internal reflection of electromagnetic radiation along the curved boundary surface of the resonator. The evanescent field of the WGM with a characteristic length of tens to hundreds of nanometers is sensitive to the refractive index change of the surrounding medium or to the binding of biological/chemical molecules to the resonator surface. A resonance frequency shift of the WGMs is induced when such events happen. The light–matter interaction is enhanced due to the long interaction length of the optical resonances associated with high-quality-factor (Q) WGMs. The high Q-factor is also correlated with narrow linewidths, which provide WGM-based sensors with high sensitivity when relying on a resonance frequency shift method of detection. Arnold *et al* [1, 2] have demonstrated the detection of protein molecules within an aqueous solution utilizing the refractive index change of the solution as measured by the shift of WGMs in silica microspheres. Quan and Guo [6] proposed and analyzed the detection of a single molecule via WGM frequency shift. Armani *et al* [8] also proved label-free single molecule detection with a micro-toroid resonator in aqueous solution, extending the technique to a dynamic range of 10^{12} in concentration. Krioukov *et al* [5] demonstrated a sensor based on integrated optical microcavities which can measure a change of as little as 10^{-4} in the refractive index of the surrounding medium.

Few prior studies have explored WGM resonances for gas-phase molecular detection. Rosenberger *et al* [9] have proposed and studied an approach of cavity-enhanced laser absorption spectroscopy using WGM for gas detection. However, only centimeter path lengths were achieved which resulted in 10^4 ppm detection levels for very strong infrared

[1] Author to whom any correspondence should be addressed.

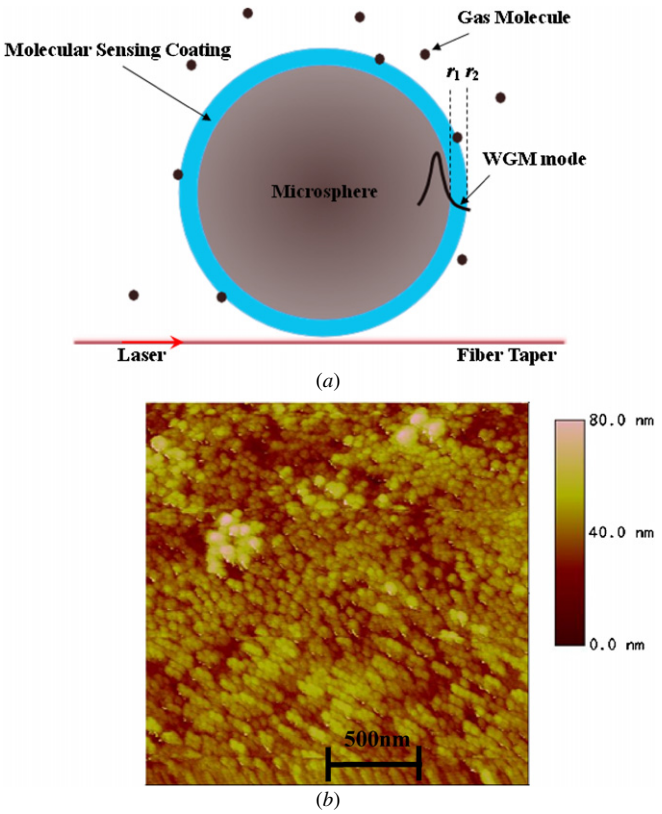

Figure 1. (*a*) Illustration of the WGM gas-sensing method with a coated microsphere. (*b*) AFM image of the film composed of 20 monolayers of 20 nm nanoparticles.

molecular absorption transitions. Locking and tuning of the WGM resonances through the spectral width of the gas absorption line proved challenging, and limited the temporal response and accuracy of the technique.

For any potential evanescent-wave absorption-spectroscopy-based WGM gas sensor, a relatively large evanescent tail of the WGM is needed for high-sensitivity concentration measurements. As the size of the evanescent tail is inversely proportional to the resonator diameter, this favors smaller resonators. However, the potential-loaded Q-value that is proportional to the path length the light travels decreases drastically as the resonator's size decreases. Thus, making a small, tunable micro-resonator with ultra-high-Q is desired; however, producing such a spherical resonator with capabilities sufficient for ppm level detection of species is challenging.

In this work, we explore a potential WGM gas-sensing method that uses a coated silica microsphere. The coating is designed to specifically adsorb only the probed gas molecules and be transparent to the laser wavelength used. The concept of coated microsphere gas sensing is illustrated in figure 1(*a*). The refractive index of the coating changes as it adsorbs gas molecules at different concentration levels, which induces a resonance frequency shift of the WGM. The complexity of resonant absorption spectroscopy is avoided in this kind of method as the WGM resonances can be read using any laser frequency, as it is not required to be resonant with an optical transition associated with the molecule of interest. Furthermore, the measurement sensitivity is determined both by the size of the wavelength shift that can be resolved by the WGM peak and the sensitivity of the coating to the analyte species.

We have designed and fabricated an optical resonator that is coated with a nanostructured layer of SiO_2 nanoparticles to study the response of the WGM spectral shift to water vapor concentration. The most prominent merit of SiO_2 as a humidity sensing material is its compatibility with the current microelectronics industry. The response and recovery times of the SiO_2 films are several milliseconds, making them well suited to performing time-resolved measurements [10]. However, most prior works have demonstrated reliable detection of water vapor concentration in excess of 20% [11] relative humidity (RH) at atmospheric pressure and room temperature. For example, Viegas *et al* [12] recently demonstrated a humidity sensor based on a long-period fiber grating coated with a thin film of SiO_2 nanoparticles, which can measure a RH range of 20–80%. For a long-period fiber-grating device described in that work, we estimate the minimum humidity detectivity of that detection strategy to be on the order of 1% RH [12]. In our study, utilizing a similar hydrophilic coating applied to a microsphere resonator, the WGM spectral shift response to water vapor concentration from 0% to 10% RH was measured to far exceed the previous minimum detectivity reported for a nanostructured SiO_2 coating.

2. Experimental setup and methods

The microsphere is made from fusing the tip of a silica single-mode bare fiber (Corning SMF-28). A fiber taper is used as a near-field coupler for both light delivery to and transmission signal from the microsensor. The fiber taper is fabricated by heating and stretching the same kind of single-mode bare fiber. High-quality microspheres with diameters between 400 and 500 μm and adiabatic fiber tapers with negligible transmission loss are prepared for the experiments. The details of sphere and taper manufacturing and quality examination can be found in [3]. We adopted the technique of electrostatic self-assembly (ESA) for fabricating the SiO_2-nanoparticle-based film [10], which has the advantages of both self-assembly and molecular control of the structure of the coating, molecular layer by molecular layer. A microsphere, 230 μm in radius formed on the tip of a fiber, is introduced to a piranha acid solution (70% H_2SO_4, 30% H_2O_2) for 10 min to create a charged surface. Then, it is suspended in a magnetic stirrer and thoroughly washed in agitated de-ionized (DI) water for 5 min. After that, the microsphere is dipped into a colloidal suspension (LUDOX TM-40, diluted to 25 mg ml^{-1}) of dissolved silica particles with an average diameter of 22 nm at pH 2.0 for 15 min to form a film of SiO_2 particles on the microsphere surface. After a similar DI water bath to remove excess adsorbed material, the microsphere is immersed for 15 min into a similar SiO_2 nanoparticle solution but with pH 10.0 so that another monolayer of SiO_2 is formed. The microsphere is again cleaned with DI water. This process is repeated until 20 overlays of the nanoparticles are coated on the microsphere

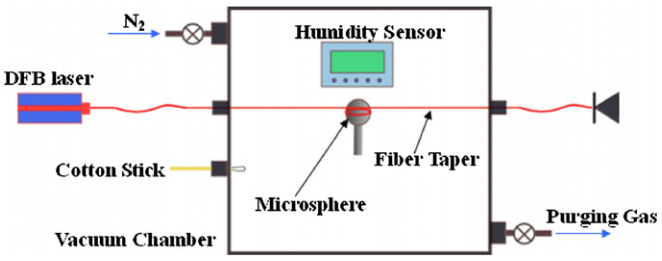

Figure 2. Experimental setup of the very low humidity (0–10%) sensing.

to form a thin film. The thickness of the film is approximately 330 nm according to a similar study of ESA-based fabrication of a similar multi-layer structure conducted by Corres *et al* [10], who used a nano-Fabry–Perot measurement to determine the layer thickness. The refractive index of the film is approximately 1.22 according to a simulation by Villar *et al* [13] and increases as it absorbs water vapor.

Figure 1(*b*) shows an atomic force microscopy (AFM) image of the surface morphology of the nanostructured coating on the microsphere. The high surface porosity and roughness enhance the behavior of the film to the super-hydrophilic regime. The contact angle of this film as fabricated onto a glass slide is measured to be less than 5°, which indicates the super-hydrophilic property of the coated surface. Prior works have investigated water adsorption and desorption process into this type of nanoporous network associated with the SiO_2 nanostructured coating. It is widely accepted that the adsorption of water can be divided into two important steps. The first step at very low humidity levels occurs when specific adsorption occurs onto hydroxyl groups through hydrogen bond (–H) interactions followed by the formation of sub-monolayer coverage. In the second step of water vapor adsorption, capillary condensation leads to a multilayer deposition of water [14]. Owing to differences in the nucleation and evaporation mechanisms inside the nanoporous network, the adsorption isotherm can show a significant hysteresis phenomenon that is mainly attributable to the capillary condensation phenomena.

Following fabrication, the coated microsphere is positioned in contact with a fiber taper inside a vacuum chamber (inner dimensions 25.4 cm × 25.4 cm × 19 cm) as shown in figure 2. The fiber is fed into the chamber using a modified tube fitting [15] to ensure a high vacuum seal around the optical fiber as it traverses though the vacuum chamber wall. A commercial RH sensor (Omega OM-DVTH) with a 10 s time constant and ±2% RH accuracy is placed 3 cm inside the microsphere to measure and record humidity changes near the WGM location inside the chamber. Dry nitrogen purging for several hours is used to decrease the humidity in the vacuum chamber to nearly 0% (within the accuracy of ±2% of the commercial RH sensor). A water vapor source (wet cotton stick) is then inserted into the chamber through another port to increase the humidity in the chamber in a controlled manner through evaporation. Laser light from a tunable DFB laser diode (1653 nm) is coupled into the coated microsphere for WGM by evanescent coupling from the adiabatic fiber taper. The tunable laser repeatedly scans across a wavelength range of approximately 170 pm using sawtooth current modulation to resolve the spectral location of the WGM as a function of the changing environmental parameters. The WGM spectral positions are recorded at the output end of the fiber taper by detection of the transmitted light intensity as a function of time, which is then temporally correlated with the wavelength modulation of the laser.

3. Results and discussion

As studied by Teraoka and Arnold [16], the evanescent field-penetration depth from an uncoated microsphere increases with higher radial mode. For higher mode orders, a greater fraction of mode energy exists in the surrounding medium. It was also found in their study that for a uniform change of refractive index in the surrounding medium, the induced resonance shift would be greater for the higher-order modes, which results in a higher sensitivity to refractive index changes. For coated microspheres, knowledge of the evanescent wave penetration depth and its relation to the radial mode number as well as to the sensitivity of the coated WGM sensor is crucial to understanding the experimental results.

The radial distribution of the transverse electronic (TE) WGMs in the coated microsphere can be described by Mie theory [16, 17]:

$$E_{l,n} = \begin{cases} A\psi_l\left(n_1 k_0^{(n)} r\right) & (r \leqslant r_1) \\ C\psi_l\left(n_2 k_0^{(n)} r\right) + D\chi_l\left(n_2 k_0^{(n)} r\right) & (r_1 \leqslant r \leqslant r_2) \\ B\chi_l\left(n_3 k_0^{(n)} r\right) & (r_2 \leqslant r), \end{cases} \quad (1)$$

where a Ricatti–Bessel function $\psi_l(z) = z j_l(z)$ and a Ricatti–Neumann function $\chi_l(z) = z y_l(z)$ are defined by use of lth spherical Bessel and Neumann functions $j_l(z)$ and $y_l(z)$, respectively. The refractive indices of the microsphere, coating and surrounding gas are described by n_1, n_2 and n_3. The terms r_1 and r_2 represent the radius of the original microsphere and the coated microsphere, respectively. $k_0^{(n)}$ is the amplitude of the wave vector in vacuum for the nth-order radial WGM. By matching the boundary conditions, the constants A, B, C and D can be determined, and the resonance wavelength can be established for a specific polar mode number l and radial mode number n. Figure 3 depicts the light intensity for the first- and fifth-order radial modes propagating by total internal reflection in a coated microsphere in the absence of analyte adsorption. It is shown that the higher radial mode penetrates deeper outside the original microsphere surface. The evanescent fractions of energy outside the original microsphere are 0.426% and 0.393% for the fifth- and first-order radial modes, respectively. Additionally, the evanescent fractions of energy in the coating are 0.379% and 0.358% for the fifth- and first-order radial modes, respectively. Thus, in our coated microspheres, higher radial modes posses both higher energy fractions in the coating and outside the original sphere. Thus, the fifth-order mode is expected to have a slightly better refractive index sensitivity (∼6% larger) in the coating than the first-order mode, as shown in figure 4.

After examining the role of radial order in sensitivity, experimental measurements of the water vapor sensitivity

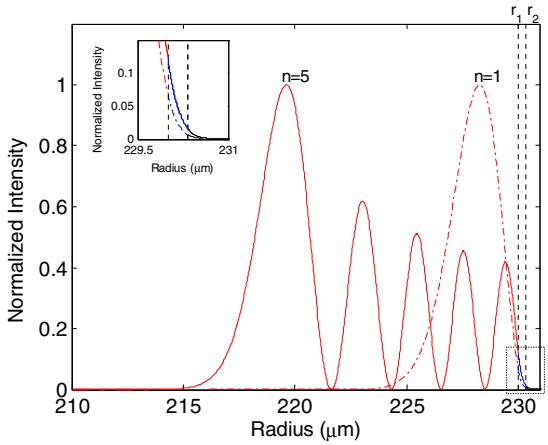

Figure 3. Intensity distribution of two TE WGMs ($n = 1$, $l = 1264$, dashed and $n = 5$, $l = 1216$,) with $r_1 = 230$ μm and $r_2 = 230.33$ μm. The dashed lines show the boundaries of the 330 nm thick coating. Refractive indices: $n_1 = 1.4862$, $n_2 = 1.22$, $n_3 = 1.0$. The inset shows the evanescent tail of the two radial modes in more detail.

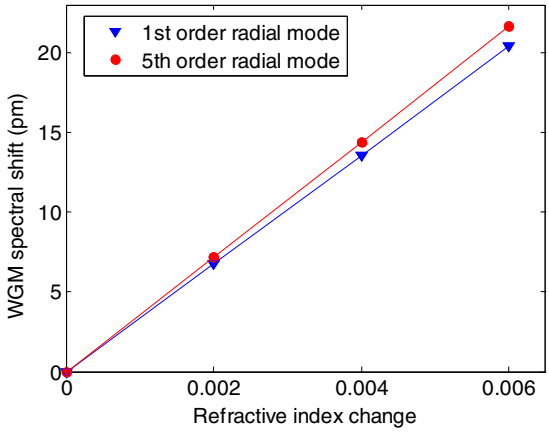

Figure 4. Simulation of the WGM spectral shift versus the refractive index change of the coating.

of the WGM associated with the coated microsphere were performed in the vacuum chamber under controlled humidity variation. As shown by the inset of figure 5, the RH in the chamber decreases slowly from 10% to 0% at temperature $T = 298.2$ K in 9140 s by slow dry nitrogen purging, and then increases back to 10% slowly in 4120 s by the insertion of a humidity source. This process is slow enough to ensure that the temporal response of the commercial humidity sensor is sufficient to fully resolve the humidity changes. In addition, the relatively long time for humidity changes allows for a spatially uniform humidity environment to be maintained in the chamber through diffusion.

As the humidity of the chamber decreases, the water desorbs from the pre-hydrated nano-structured silica film, causing the effective refractive index of the coated layers to decrease, hence blue-shifting the WGM resonance wavelength. Once the chamber humidity reaches the minimum value, the water vapor source increases the humidity and the water begins to be adsorbed by the nano-structured silica film, starting from sub-monolayer coverage and progressing to physisorption of bulk water into the film. As the water

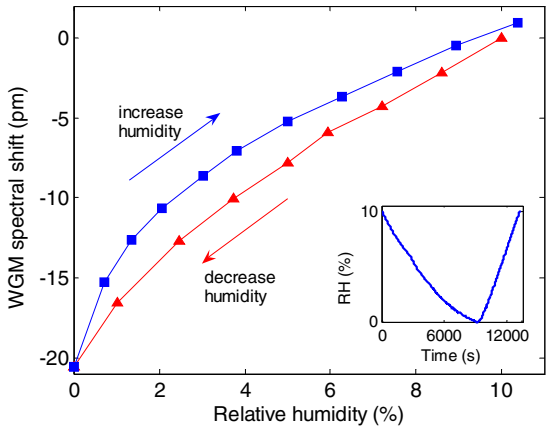

Figure 5. WGM spectral shift versus RH change at 298.2 K; inset: humidity change versus time.

occupies the nanoporous network, the effective refractive index is increased, while the resonance of the WGM shifts to larger wavelengths. The temperature inside the chamber is maintained at 298.2 ± 0.1 K during the test, as measured by the commercial sensor (0.01 K resolution).

To obtain the WGM temperature sensitivity of this coated microsphere in the humidity test, the RH is kept at a constant of 5% and the spectral shift is measured against a temperature change of 297.7 K to 298.7 K in the chamber. The sensitivity to temperature changes is 13.2 ± 0.01 pm K^{-1}, which correlates with that measured previously in [4], showing that the thin coating does not significantly affect the overall temperature sensitivity of the micro-resonator. The spectral shift of a randomly selected, strongly coupled WGM versus RH is shown in figure 5, corrected for any temperature variations during the test. As shown in figure 4, the sensitivity of the fifth-order mode is only 6% higher than that of the first-order radial mode in a shift of 20 pm (RH change of 10%). Since the tested WGM has a radial mode order less than fifth order confirmed by a wider range laser tuning observation, this small difference can be neglected when comparing with the experiment result. In this experiment, the WGM spectral shift is approximately 16 pm during the humidity loading phase and 18 pm during the humidity unloading phase, which corresponds to the refractive index changes of 0.0046 and 0.0052 RIU, respectively, as shown in figure 4. Therefore, the method has a sensitivity of 2.9×10^{-4} RIU pm^{-1} of spectral shift. The optical shift measured with humidity change is reproducible to within the precision of the commercial RH sensor.

The minimum detectivity of this technique depends upon the ability to determine small spectral shifts relative to the initial position, which is dependent on the Q-factor of the coated microspheres. The Q-factor of the WGM used in this study is 0.8×10^6. From prior experience, a shift of 1/100 of the related linewidth can be easily resolved by the detection scheme employed, which correlates to a spectral shift sensitivity in the range of ∼0.02 pm. Using the sensor responsivity at very low humidity (0.02 pm/ppm H_2O) to estimate the minimum detectivity, a change of 1 ppm H_2O (0.003% RH) should be resolvable using the coated WGM microspheres. A finer resolution could be achieved if such

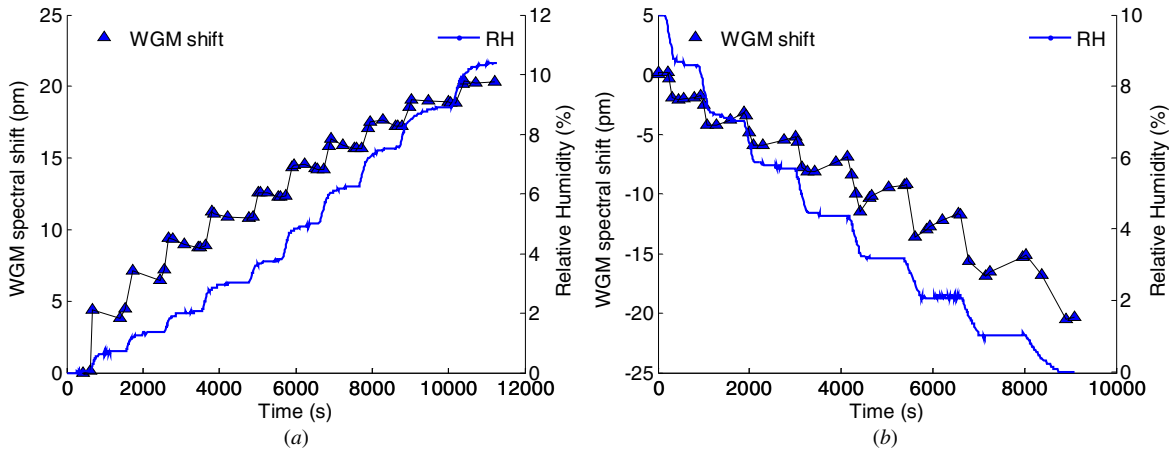

Figure 6. WGM spectral shift with a continuous step change of humidity at 300 K: (*a*) humidity step increase; (*b*) humidity step decrease.

a coated microsphere is fabricated with a higher Q-value; however, limitations in our fabrication process typically limit the maximum achievable Q-value to less than 10^9. The coated microsphere geometry represents a significant enhancement of low-humidity detection when compared to long-period fiber-grating methods that employ similar coatings. In addition, we can see that the coating behaves similarly in the spherical geometry for the microsphere and the cylindrical geometry for the fiber-optic sensors as the humidity sensitivity of the coating is measured to be 5.8×10^{-6} RIU/ppm H_2O in this study as compared to the range of 3–8 $\times$ 10^{-6} RIU/ppm H_2O as demonstrated by Viegas *et al* [12].

Separation between the sensitivity of the coated WGM microsphere during the humidity loading and unloading process is seen, suggesting a significant hysteresis effect, as shown in figure 5. This likely results from the fact that mechanisms for the adsorption and desorption of water molecules for the super-hydrophilic coating are considerably different and not exactly inverse of each other. To study the dynamic transport of water molecules between the thin nano-coating and the surrounding environment, a calibration test with continuous step changes of humidity is performed. To create a fast change in RH, the water vapor source is exposed to the vacuum chamber for approximately 10 s using a valve and then quickly isolated from the chamber to create the step humidity increase. An equivalent step humidity decrease is achieved by short-duration dry nitrogen purging. Step changes in humidity values were easily reproducible by this method to within the accuracy of the commercial RH sensor. The time constants for these step changes were approximately 200 s for increasing humidity and 300 s for decreasing humidity. The mixing timescales are large due to the reliance on diffusion to mix the introduced water vapor into the cell. However, due to the small physical separation between the commercial RH sensor and the WGM device, the humidity value at both locations is assumed to be the same for the long time scales used in this study. Temperature variation is maintained within 0.08 K and the effect of temperature variation is corrected for in all test results. As shown in figure 6, the WGM spectral shift appears to exhibit two distinct dynamic phenomena in response to the step variation in environmental humidity. The WGM shift closely follows the initial step change of the humidity suggesting prompt adsorption and desorption of water molecules to and from the nano-coating. This fast-response time constant (<1 s) of the nano-coating was one of the primary reasons why it was selected for humidity measurement by our and other research groups. However, there also appears to be a long time-constant process (∼700 s), which seems to counteract the refractive index change of the nano-coating.

Figure 6 shows that after an initial step change in the WGM spectral position, the resonant wavelength slowly relaxes to an intermediate value. This phenomenon indicates that the dynamic adsorption and desorption processes tend to return to the initial water concentration level in the coating when the source for sustaining the humidity gradient is removed, even though the humidity in the vacuum chamber remains constant. In addition, this shift retraction phenomenon is more significant at lower humidity levels.

For further investigation, we examined the stability of the WGM shift as a dynamic process when a near step change in humidity is created in the chamber. As shown in figure 7(*a*), the spectral shift promptly increases due to the rapid change in humidity. However, the spectral shift then begins to decrease and tends to a constant value within 1000 s after a single humidity increase step change. The final spectral shift level is still significantly higher than the initial level. When performing the same type of step change test for decreasing humidity levels (figure 7(*b*)), the spectral shift follows the commercial sensor very well for the first 500 s of the test. However, the long time-scale behavior shows that the spectral shift nearly returns to its initial level over a very long time period (>3000 s) for the decreasing step change in humidity. We can conclude that the spectral shift for the nano-coated WGM microsphere depends on its prior humidity history in addition to the gradual drift shown in figure 7 associated with some slower dynamic process. Clearly, desorption and adsorption are complex processes for this kind of coating at lower humidity levels and their effects on the sensitivity, stability, and temporal accuracy of nano-coated WGM microspheres preclude further development of

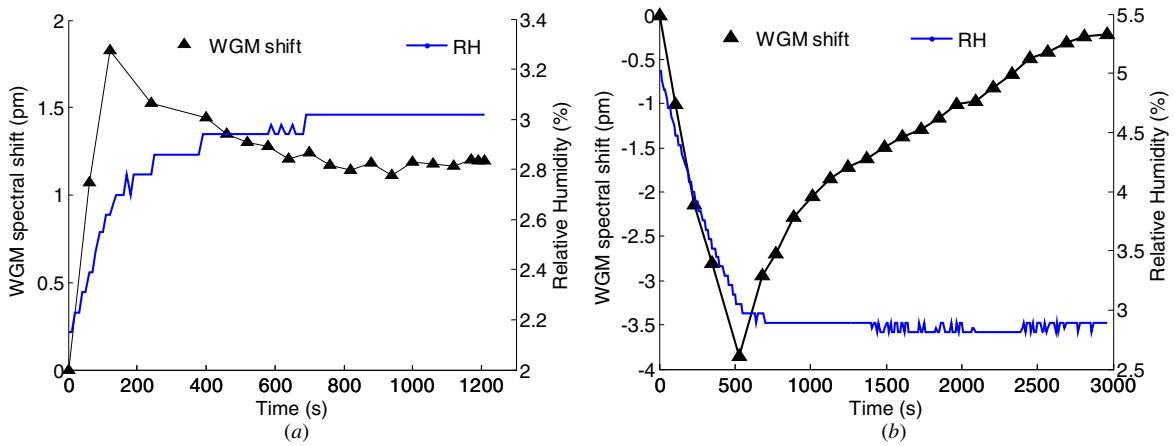

Figure 7. WGM spectral shift with a single step change of humidity at 300 K: (*a*) humidity step increase; (*b*) humidity step decrease.

this concept into a steady humidity sensor for the low RH range. The sensing methodology appears to be better suited to dynamic humidity measurements where the measurement time scale involved is less than 100 s.

The physical phenomenon which gives rise to the multiple time constants seen in figure 7 is also responsible for the hysteresis behavior shown in figure 5. Due to the behavior of the complex water vapor desorption process from the coating during the periods of humidity decrease and its extremely long time constant, the sensitivity of the coated WGM microsphere during decreasing humidity conditions is much lower than that of the increasing humidity environment. If the humidity changes occurred over much faster time scales (with changes on the order of 10 s or less), the two curves in figure 5 would display similar sensitivities and exhibit a much better overlap.

4. Conclusion

In summary, we have analyzed the WGM spectral shift induced by a refractive index change in a transparent coating by Mie theory. We have also presented experimental results of the spectral shift response of optical WGMs for a SiO_2 nanoparticle-coated microsphere in response to environmental humidity changes. Significant response using the nano-SiO_2 particle coating is achieved at a very low humidity level (<10%), which far exceeds the sensitivities reported by prior efforts. However, the coating appears to exhibit poor stability due to its demonstrated significant hysteresis effect and long effective time constant. The dynamic adsorption and desorption processes of water molecules interacting with this coating are revealed by the WGM spectral shift during the step changes in humidity. The water concentration in the coating tends to return to its initial value when the source for the humidity gradient is removed even though the chamber humidity remains constant. However, this study clearly shows the merit of optical resonance methods as a useful measurement technique for determining surface interactions and transport dynamics within thin film coatings.

Acknowledgments

The authors acknowledge the laboratory support of the coating process from Professor Denhardt (Rutgers University, Department of Biology) and the AFM imaging support from Professor Qingrong Huang (Rutgers University, Department of Food Science). ZG acknowledges partial support to the work by the National Science Foundation under grant no CBET-0651737 and by the US Department of Agriculture under CSREES award 2008-01336. TR acknowledges support for the work from Rutgers University Academic Excellence Fund.

References

[1] Vollmer F, Braun D, Libchaber A, Khoshsima M, Teraoka I and Arnold S 2002 Protein detection by optical shift of a resonant microcavity *Appl. Phys. Lett.* **80** 4057–9

[2] Vollmer F, Arnold S, Braun D, Teraoka I and Libchaber A 2003 Multiplexed DNA quantification by spectroscopic shift of two microsphere cavities *Biophys. J.* **85** 1974–9

[3] Ma Q, Rossmann T and Guo Z 2008 Temperature sensitivity of silica micro-resonators *J. Phys. D: Appl. Phys.* **41** 245111

[4] Ma Q, Rossmann T and Guo Z 2010 Whispering-gallery mode silica microsensors for cryogenic to room temperature measurement *Meas. Sci. Technol.* **21** 025310

[5] Krioukov E, Klunder D, Driessen A, Greve J and Otto C 2002 Sensor based on an integrated optical microcavity *Opt. Lett.* **27** 512–4

[6] Quan H and Guo Z 2007 Simulation of single transparent molecule interaction with an optical microcavity *Nanotechnology* **18** 375702

[7] Sumetsky M, Windeler R, Dulashko Y and Fan X 2007 Optical liquid ring resonator sensor *Opt. Express* **15** 14376–81

[8] Armani A, Kulkarni R, Fraser S, Flagan R and Vahala K 2007 Label-free, single-molecule detection with optical microcavities *Science* **317** 783–7

[9] Farca G, Shopova S and Rosenberger A 2007 Cavity-enhanced laser absorption spectroscopy using microresonator whispering-gallery modes *Opt. Express* **15** 17443–8

[10] Corres J, Matias I, Hernaez M, Bravo J and Arregui F 2008 Optical fiber humidity sensors using nanostructured coatings of SiO_2 nanoparticles *IEEE Sensors J.* **8** 281–5

[11] Chen Z and Lu C 2005 Humidity sensors: a review of materials and mechanisms *Sensor Lett.* **3** 274–95

[12] Viegas D, Goicoechea J, Corres J, Santos J, Ferreira L, Araujo F and Matias I 2009 A fibre optic humidity sensor based on a long-period fibre grating coated with a thin film of SiO_2 nanospheres *Meas. Sci. Technol.* **20** 034002

[13] Villar I, Matías I, Arregui F and Claus R 2005 Fiber-optic hydrogen peroxide nanosensor *IEEE Sensors J.* **5** 365–71

[14] Wang C, Wu C, Chen I and Huang Y 2005 Humidity sensors based on silica nanoparticle aerogel thin films *Sensors Actuators* B **107** 402–10

[15] Abraham E and Cornell E 1998 Teflon feedthrough for coupling optical fibers into ultrahigh vacuum systems *Appl. Opt.* **37** 1762–3

[16] Teraoka I and Arnold S 2006 Enhancing the sensitivity of a whispering-gallery mode microsphere sensor by a high-refractive-index surface layer *J. Opt. Soc. Am.* B **23** 1434–41

[17] Johnson B 1993 Theory of morphology-dependent resonances: shape resonances and width formulas *J. Opt. Soc. Am.* A **10** 343–52